Sustainable Energy & Fuels

ROYAL SOCIETY OF CHEMISTRY

PAPER

View Article Online
View Journal | View Issue

Cite this: *Sustainable Energy Fuels*, 2025, **9**, 1859

Saline microalgae cultivation for the coproduction of biofuel and protein in the United States: an integrated assessment of costs, carbon, water, and land impacts†

Jingyi Zhang, *[a] Yunhua Zhu,[b] Troy R. Hawkins,*[a] Bruno C. Klein,[c] Andre M. Coleman,[b] Udayan Singh,[a] Ryan Davis,[c] Longwen Ou,[a] Yiling Xu,[b] Saurajyoti Kar,[a] Matthew Wiatrowski,[c] Song Gao[b] and Peter Valdez[b]

The development of microalgal biorefineries, utilizing high-value coproducts, offers a strategy to lower biofuel production costs, while the use of saline-tolerant microalgal species contributes to reducing freshwater consumption. This study evaluates the life cycle performance of saline microalgae cultivation and conversion at a national scale by analyzing economics, greenhouse gas (GHG) emissions, marginal GHG avoidance cost (MAC), water scarcity footprints, land-use change emissions, and resource availability. The Algal Biomass Assessment Tool (BAT) is applied for site selection, while algae farm and conversion models are used for techno-economic analysis (TEA). The Greenhouse Gases, Regulated Emissions, and Energy use in Technologies (GREET) model is employed for life cycle assessment (LCA) by integrating the outputs from BAT and TEA. Our findings demonstrate that electricity and nutrient consumption are the primary drivers of base case GHG emissions, while biomass yield is the key factor determining both GHG emissions and economic performance. Saline microalgal biorefineries can achieve a MAC limit of $80–200/tonne when high-value bio-coproducts, such as whey protein concentrate, are benchmarked, contingent on supply-demand conditions and other market drivers. However, this reduction may not be compatible with current carbon prices. Further increase in biomass yield, reductions in energy and nutrient usage, and the careful selection of high-value protein coproduct targets with high conventional GHG emissions during the design stage are recommended. Additionally, saline microalgal biorefineries show great potential in addressing water stress, as the electricity requirements for desalinating brackish and saline water are relatively low compared to the overall system electricity demand.

Received 12th October 2024
Accepted 17th February 2025

DOI: 10.1039/d4se01423e

rsc.li/sustainable-energy

Introduction

Numerous studies highlight the need for sustainable and cost-effective bioenergy solutions that do not exacerbate water scarcity or encroach upon valuable farmland.[1,2] In this context, microalgal biorefineries—integrated systems designed for the large-scale cultivation, harvesting, and processing of microalgae to produce fuels, chemicals, and high-value added commodities—have emerged as a potential solution.[3] Microalgae can be cultivated on marginal lands, avoiding competition with arable lands, and their high photosynthetic efficiency allows for greater biomass and fuel/product generation per unit area compared to other biomass feedstocks. Additionally, their adaptability to diverse water sources, including saline and wastewater, presents a strategic advantage in conserving freshwater resources, especially in areas facing water shortages.[4]

However, the commercial production of biofuels from microalgae faces significant challenges, such as the high capital investment required for algae farms and the substantial energy needed for cultivation and harvesting.[5] In the United States, the projected decline in conventional fuel prices further challenges the competitiveness of microalgal and other alternative biofuels.[6] Moreover, depending on the cultivation conditions, algal systems can consume more freshwater than incumbent sources of fuel production.[7]

Recent studies suggest that incorporating coproduct revenues can improve the financial viability of algal fuel systems.

[a]*Systems Assessment Center, Energy Systems and Infrastructure Analysis Division, Argonne National Laboratory, Lemont, IL 60439, USA. E-mail: trh@alumni.cmu.edu; jingyi.zhang@anl.gov; Tel: +1-(630)252-6428; +1 630-252-1381*

[b]*Pacific Northwest National Laboratory, 902 Battelle Blvd, Richland, WA 99352, USA*

[c]*Catalytic Carbon Transformation & Scale-up Center, National Renewable Energy Laboratory, Golden, CO 80401, USA*

† Electronic supplementary information (ESI) available. See DOI: https://doi.org/10.1039/d4se01423e

Relevant coproducts include bioplastics, animal feed, and naphtha.[8–11] Additionally, life cycle assessments (LCAs) of algal biofuel production indicate that electricity generation and succinic acid production as coproducts can significantly reduce greenhouse gas (GHG) emissions.[12,13] Previous studies discussed the water demand and stress impacts of microalgal biorefineries, which vary significantly by location.[14,15]

Building on our previous "2022 Algae Harmonization Update" study that examined the resource availability, economic, and environmental performance of saline microalgal biorefineries producing fuels and protein bioproducts,[16] this study aims to: (1) providing a comprehensive life cycle performance evaluation for biorefineries that coproduces fuel and protein products and examining trade-offs between carbon emission reduction and cost by using the marginal GHG avoidance cost (MAC); (2) identifying the interrelationship between water stress and other life cycle performance parameters; (3) examining the impact of land use on environmental outcomes; and (4) introducing chicken meat as another benchmark target for algal bio-coproduct, offering additional benchmarks to high-protein products, since the prior study focused on whey and soy protein concentrate (PC) targets.

System description and method

This section is divided into two main parts: system description and methods, supplemented by additional assumptions and parameters listed in the ESI.† The system description provides details of the microalgal biorefinery processes for fuel and bio-coproduct production. The methods section includes the following components: (1) Goal and scope definition:defines the study's scope, system boundary, and functional units. (2) Site selection: explains the site selection process based on the Biomass Assessment Tool (BAT) model. (3) Biorefinery-level minimum selling prices (MSPs) and GHG emissions: describes the use of techno-economic analysis (TEA) and LCA to calculate MSPs and GHG emissions at the biorefinery level. (4) Selling prices (SPs) and GHG emissions from conventional systems: details the sources of selling price (SP) and GHG emission values used for benchmarking. (5) Market considerations for microalgal PC: illustrates the uncertainties and assumptions in introducing microalgal PC into the market. (6) MAC: explains how MAC evaluates trade-offs between TEA and LCA results. (7) Water scarcity footprint (WSF): illustrates the calculation of quality- and quantity-based WSF using a mathematical model. (8) Direct land use change (DLUC) and indirect land use change (ILUC) calculations: introduces the definitions and considerations of DLUC and ILUC in this study.

System description

Fig. 1 illustrates the processes within the system boundary, which includes three main components: CO_2 capture and transport (Section 1.1 in the ESI†), algae cultivation and harvesting (Section 1.2 in the ESI†), and algae conversion to fuel and protein coproducts *via* hydrothermal liquefaction (HTL) (Section 1.3 in the ESI†). CO_2 is captured from various sources (Table S2 in the ESI†), then transported to open ponds. Algae are cultivated in these ponds using captured CO_2 and nutrients, harvested, dewatered, and stored seasonally to ensure consistent conversion throughput. Groundwater with a salinity of 40 000 mg L^{-1} TDS or less is delivered to cultivation ponds, with an FO membrane unit processing pond blowdown water to regulate salinity. The concentrated brine from the FO membrane unit is disposed of *via* deep well injection. Two downstream processing cases are analyzed: fuel-only and fuel with protein coproduction. In the fuel-only case, algae slurry undergoes HTL to produce biocrude, which is upgraded to sustainable aviation fuel (SAF), diesel, and naphtha. In the fuel and protein coproduction case, algae are first processed for protein extraction before HTL, with subsequent outputs handled similarly. Potential bioproducts are benchmarked with soybean PC, whey PC, and chicken meat. Digestible protein is selected as the basis for estimating the replacement ratio of algae PC to benchmark the three protein targets. More detailed information can be found in Section 1.4 in the ESI.† Herein, this study examines four cases: fuel-only production, fuel and PC production benchmarking soybean PC, fuel and PC production benchmarking whey PC (60% protein content), and fuel and PC production benchmarking chicken meat. Key parameters and assumptions are summarized in Table S1.†

Methods

Goal and scope definition. This study follows ISO 14040 and 14044 guidelines for LCA. The system boundary encompasses everything from raw material extraction to fuel combustion (well to wheel). It is assumed that infrastructure construction has a negligible contribution to the GHG emission results,[17] and it is excluded from the inventory. The biorefinery-level LCA approach is selected to represent the environmental impacts of the biorefinery which coproduces fuel and other value-added coproducts. This approach can avoid arbitrary decisions related to the allocation method or the choice of evaluation of metrics tied to a specific product by using displacement method. The MSPs are normalized to 1 gallon of gasoline equivalent (GGE) of fuel production in the fuel-only case and to 1 GGE of fuel plus 5.9 kg of PC production in fuel and PC coproduction cases. The functional unit for GHG emissions is defined as 1 MJ of fuel production in the fuel-only case and as 1 MJ of fuel plus 0.05 kg of PC production in the fuel and PC coproduction cases. The two units are interchangeable using 120 MJ/GGE but are not standardized between MSPs and GHG emissions, facilitating comparisons with literature data. Specifically, MSPs for fuel production are typically expressed in dollars per GGE or liter,[7,9,10] while GHG emissions are reported in g CO_2-eq. per MJ.[18] Retaining these commonly used units in TEA and LCA studies would enhance comparability. Additionally, to provide different perspectives for fuel and protein coproduction systems and allow comparison with fuel-only or protein-only systems, the MSPs per GGE of fuel production by accounting for protein selling credits and GHG emissions per MJ of fuel production and per kg of PC production by using the economic allocation method are available in Section 6 in the ESI.†

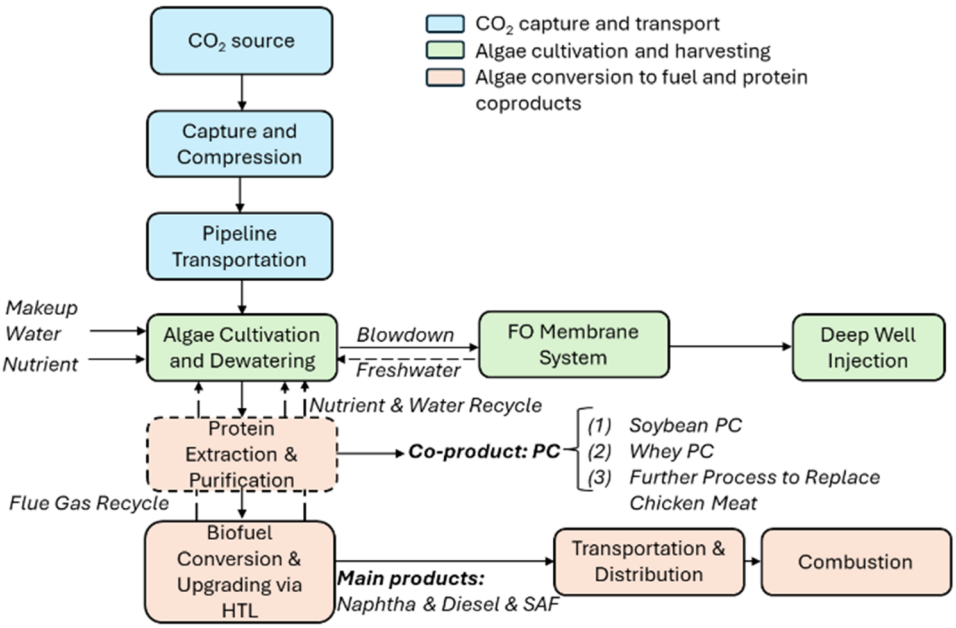

Fig. 1 System boundary flow diagram (dashed box: the protein extraction and purification process applies only to cases involving fuel and protein coproduction).

Site selection. The BAT[14,19] is utilized to down-select saline microalgal sites by integrating geospatial and biophysical modeling approaches. BAT enables the prediction of cultivation outcomes based on each site's unique environmental conditions, with sites selected that can most plausibly achieve the Bioenergy Technologies Office's 2030 goal of a daily productivity of 25 g ash-free dry weight (AFDW) per m^2 per day.[20] Additionally, CO_2 sources are identified using various databases and data collections.[21–24] CO_2 source proximity influences site selection, with a cost cap of $75 per tonne applied for CO_2 logistics. The outputs from the BAT model, including site area, monthly biomass productivity, and costs for CO_2 delivery, makeup water sourcing, pipeline distance, salinity management, and saline pond blowdown, are integrated into an algae farm TEA model based on site-specific details and configurations, and ultimately determines the minimum biomass selling price (MBSP). Further details can be found in the previous study.[16]

Biorefinery-level MSPs and GHG emissions. Biorefinery-level MSPs and GHG emissions are evaluated to quantify the total cost and GHG emissions to produce all finished products in the biorefinery, providing a comprehensive overview of the biorefinery's performance relative to conventional systems.[25]

MSPs are calculated using a discounted cash flow rate of return method by integrating the MBSP outputs from the algae farm model with the production costs and market SPs from the algae conversion model. The capital cost estimation for the algae HTL conversion system is based on previous TEA studies,[26,27] with equipment costs sourced from Aspen Process Economic Analyzer[28] and prior in-house estimates. Variable operating costs are estimated based on raw material consumption results from the conversion model, and unit prices from industrial sources and previous work.

The well-to-wheel GHG emissions are calculated using the Greenhouse gases, Regulated Emissions, and Energy use in Technologies (GREET) 2022 model.[29] GHG emissions are quantified using IPCC's Sixth Assessment Report 100 year characterization factors (fossil CH_4: 29.8; N_2O: 273). Emissions from the combustion of the produced fuel are not included in the life cycle, as these emissions would have otherwise entered the atmosphere. The life cycle inventories (LCIs) are generated from process modeling based on the outputs from BAT and TEA models and integrated into the GREET model. Detailed LCI of the system can be found in Table S6.†

The protein coproduct is benchmarked against soy and whey PC as direct replacements without further processing. In contrast, benchmarking against chicken meat requires additional energy and materials to process the protein coproduct into a chicken meat alternative. The processing cost is assumed to be the same as the material cost, as reported.[30] For the LCA, only the major components involved in processing protein coproduct for chicken meat alternatives (CMAs) are included due to data limitations. The upstream LCIs are available in Section 2.3.2 in the ESI.† It is noticeable that the cost and LCA results for processing PC to CMAs are subject to uncertainties due to data limitations.

SPs and GHG emissions from conventional products. To provide an equitable comparison between biorefinery and conventional systems, this study investigates the SPs and GHG emissions associated with conventional petroleum-based fuel, soybean PC, whey PC, and chicken meat productions. The SP for fuel is estimated using a five-year average wholesale price of $2.6/GGE for petroleum diesel, jet fuel, and naphtha, based on reported and projected values from 2022 to 2026.[6] For soybean PC, whey PC, and chicken meat, the SPs and market sizes are

obtained from different sources and summarized in Table S4 in the ESI.†

The GHG emissions from conventional fuel production are derived from the weighted-average GHG emissions of gasoline, jet fuel, and diesel (~87 g MJ^{-1}). Conventional soybean PC production involves soybean processing with coproducts like soybean hulls, oil, and molasses, with GHG emissions calculated through economic allocation based on literature.[31] Whey PC, obtained from liquid whey—a coproduct of cheese production[32]—has its GHG emissions estimated through economic allocation between cheese and liquid whey in this study.[33–35] It is important to note that the GHG emissions attributed to liquid whey, being a cheese production coproduct, warrant careful consideration since substituting whey PC with algae PC will not eliminate cheese production. Nonetheless, with rising protein demand, microalgal PC could potentially fulfill incremental demands when liquid whey falls short. GHG emissions generated from chicken meat production are sourced from the GREET model.[36] It is important to note that ILUC and DLUC are not included in the final GHG emission results. However, incorporating ILUC and DLUC can impact environmental outcomes and introduce variability. A separate discussion on land use change (LUC) is available in Section DLUC and ILUC calculation.

Factors to consider by introducing microalgal PC into the market. The microalgal PC protein content is about 72% by weight, and the coproduct PC is assumed to be suitable for human consumption due to its high protein content and the processing schematic employed in this study. Microalgae proteins hold promise as substitutes for whey and soybean PC and chicken meat, although flavor enhancement might be necessary through additional processing.[37,38] It is important to note that the potential for substitution is subject to various factors, including market demands, flavor acceptance, and social trends towards minimally processed foods. The MSPs and GHG emission calculations for fuel and protein coproduction in this study are grounded in their respective targeted protein market limits as shown in Table S4 in the ESI,† illustrating cases where the microalgal biorefinery is optimized for maximum protein coproduct yield.

MAC. The MAC evaluates the trade-offs between the SPs and GHG emissions, as detailed in eqn (1). This metric measures the additional cost incurred for each unit of CO_2 mitigated when transitioning from the reference product (petroleum fuels and conventional PC products) to the alternative product (algal fuels and PC products). Sites with GHG emissions exceeding those of conventional fuels are excluded from this analysis.

WSF. The WSF quantifies the potential water use stress, considering regional availability and demand. Both quality-based and quantity-based WSFs are incorporated into the calculation as shown in eqn (2).[39]

The quality-based WSF is calculated by multiplying water consumption by the correction factor R, which represents the hardness level required to desalinate brackish and saline water to freshwater. R is defined as the ratio of the specific energy needed for desalination to the maximum energy required at the highest salinity (40 000 mg L^{-1}) studied. The specific energy consumption (SEC) of reverse osmosis (RO) is derived from a mathematical model for a municipal-scale plant and used to represent the energy needed for desalination and to quantify the quality-based WSF.[40] RO, the most commonly used desalination method,[41] is chosen for calculating the quality-based WSF instead of FO due to the availability of SEC mathematical model. More detailed information regarding R can be found in Section 3 in the ESI.† Freshwater does not require desalination, thus the quality-based WSF of freshwater is zero.

The quantity-based WSF is calculated by multiplying the water consumption by the characterization factor (CF), which represents local water availability. Brackish and saline water are considered always abundant, giving them a CF of zero. For freshwater, the CF is derived from the AWARE-US model developed by Argonne National Laboratory.[42]

$$\mathrm{WSF}_{i,j} = \mathrm{WSF}_{\mathrm{SW},i,j} + \mathrm{WSF}_{\mathrm{FW},i,j} = R_{i,j} \times \mathrm{SWC}_{i,j} + \mathrm{CF}_{\mathrm{FW},i} \times \mathrm{FWC}_{i,j}$$

$$\mathrm{WSF}_{\mathrm{SW},i,j} = \mathrm{WSF}_{\mathrm{quality}} + \mathrm{WSF}_{\mathrm{quantity}} = R_{i,j} \times \mathrm{SWC}_{i,j} + \mathrm{CF}_{\mathrm{SW},i} \times \mathrm{SWC}_{i,j} = R_{i,j} \times \mathrm{SWC}_{i,j} \ (\because \mathrm{CF}_{\mathrm{SW},i} = 0)$$

$$\mathrm{WSF}_{\mathrm{FW},i,j} = \mathrm{WSF}_{\mathrm{quality}} + \mathrm{WSF}_{\mathrm{quantity}} = R_{i,j} \times \mathrm{SWC}_{i,j} + \mathrm{CF}_{\mathrm{FW},i} \times \mathrm{FWC}_{i,j} = \mathrm{CF}_{\mathrm{FW},i} \times \mathrm{FWC}_{i,j} \ (\because \mathrm{SEC}_{i,j} = 0)$$

$$\mathrm{CF}_{\ i} = \frac{\mathrm{AMD}_{\mathrm{US}}}{\mathrm{AMD}_i}$$

$$R_{i,j} = \frac{\mathrm{SEC}_{i,j}}{\mathrm{SEC}_{\max}} = \frac{8 \times 10^{-5} \times \mathrm{TDS}_{i,j} - 0.024}{3.296}, \quad (2)$$

when $\mathrm{TDS}_{i,j} \leq 40\,000$ mg L^{-1}.$\mathrm{WSF}_{i,j}$ – water scarcity footprint at site j in county i.$\mathrm{WSF}_{\mathrm{SW},i,j}$ – saline water scarcity footprint at site j in county i.$\mathrm{WSF}_{\mathrm{FW},i,j}$ – freshwater scarcity footprint at site j in county i.$R_{i,j}$ – correction factor at site j in county i.CF_i – freshwater characterization factor in county i.$\mathrm{SWC}_{i,j}$ – saline water

$$\text{Marginal cost of GHG avoidance} = \frac{\left(\text{Cost of alternative product}, \frac{\$}{\mathrm{MJ}}\right) - \left(\text{Cost of reference product}, \frac{\$}{\mathrm{MJ}}\right)}{\left(\text{GHG intensity of reference product}, \frac{\mathrm{g\ CO_2e}}{\mathrm{MJ}}\right) - \left(\text{GHG intensity of alternative product}, \frac{\mathrm{g\ CO_2e}}{\mathrm{MJ}}\right)} \quad (1)$$

consumption at site j in county i.$FWC_{i,j}$ – freshwater consumption at site j in county i.AMD_{US} – the national average remaining available water ($m^3\ m^{-2}$).AMD_i – remaining available water in county i ($m^3\ m^{-2}$).$SEC_{i,j}$ – specific energy consumption at site j in county i (kW h m^{-3}).SEC_{max} – maximum specific energy consumption at salinity of 40 000 mg L^{-1} (kW h m^{-3}).$TDS_{i,j}$ – total dissolved solids at site j in county i (mg L^{-1}).

DLUC and ILUC calculation. DLUC takes place when repurposing biomass for bioenergy feedstock production leads to land use changes on the same land. ILUC happens when using biomass for a new purpose, like biofuel production, leads to changes in land use elsewhere. Carbon emissions from DLUC and ILUC are important in LCA studies but are highly uncertain.[43] In this study, LUC carbon emissions are not included in the GHG emission calculations but are discussed for future research in results and discussion section. DLUC emissions from the microalgal biorefinery are estimated based on initial land use and location-specific LUC carbon emission factors,[44,45] with details in Section 4 of the ESI.† ILUC is considered when original land use is for crops or hay/pasture, necessitating alternative land use elsewhere.

For benchmarking protein coproducts, LUC emissions from conventional soybean PC, whey PC, and chicken meat production are considered. Table S16 in the ESI† summarizes literature on LUC emissions for soybean, milk, and chicken meat production, with soybeans as feedstock for soybean PC and milk for cheese and liquid whey production. The summary table provides an emissions range of LUC in conventional protein product systems.

Results and discussion

Biorefinery-level MSPs and GHG emissions

The biorefinery-level MSPs and GHG emissions are calculated and compared with SPs and GHG emissions from conventional fuel and PC production for soybean PC, whey PC, and chicken meat. Fig. 2(a) and (b) present the SPs and GHG emissions for conventional fuel and PC production. As illustrated in Fig. 2(c) and (d), when the microalgal biorefinery solely produces fuel, its MSPs cannot compete with those of conventional fuel; however, it achieves lower or comparable GHG emissions at some sites, with a potential cumulative fuel production of 12.0 billion GGE under the GHG benchmark of conventional fuel. Fig. 2(e)–(h) illustrate the MSPs and GHG emissions associated with fuel and PC coproduction. The fuel and PC coproduction cases incur higher production costs and GHG emissions than the fuel-only case. This discrepancy arises because some algal biomass is diverted away from fuel to protein coproduction, incurring extra costs and energy for protein extraction and purification.

The MSPs and GHG emissions from fuel and PC coproduction for soybean PC and whey PC are the same, reflecting identical processing steps in these two cases. While conventional whey PC has higher SP ($3.7/kg) and GHG emissions (14 kg CO_2-eq. per kg whey PC) with a smaller market size (3.5 MMT/yr), soybean PC features lower SP ($1.3/kg) and GHG emissions (0.47 kg CO_2-eq. per kg soybean PC) but a larger market size (13 MMT/yr). Compared to conventional fuel and soybean PC, microalgal fuel and PC coproduction exhibits higher SP and GHG emissions, yet it presents lower values compared to conventional fuel and whey PC in most cases, as demonstrated in Fig. 2(e) and (f). Soybean cultivation consumes significantly less energy than algae cultivation. Specifically, 0.60 kW h of process electricity and 1.8 MJ of process heat are required per kg of algae AFDW, compared to only 0.019 kW h and 0.57 MJ of heat per kg of soybean AFDW production. Comparisons of these energy and nutrient consumption metrics are detailed in Table S17 in the ESI.† Reducing energy consumption is essential to enhance the feasibility of microalgal biorefinery systems and ensure their competitiveness with highly efficient benchmarks, such as those involving soybeans. Conventional whey PC production is energy and material intensive. To produce 1 kg of whey PC (protein content 60%), 80 kg of liquid whey containing 6 wt% dry mass is required, and it commands a higher SP and incurs greater GHG emissions compared to microalgal PC and soybean PC. However, as discussed in section SPs and GHG emissions from conventional products, substituting whey PC with algal PC does not eliminate cheese production; this benchmark is viable only when the supply of liquid whey is insufficient to meet that demand.

The coproduction case for CMAs requires additional energy and materials to convert algal PC into meat substitutes, where 1 kg of CMAs includes 0.3 kg of algal PC, 0.1 kg of soybean PC, and other ingredients for flavoring based on personal communication with an expert in the area.[46] Chicken meat, with a SP of $1.6/kg and GHG emissions of 4.7 kg CO_2-eq. per kg, falls between soybean PC and whey PC in terms of cost and emissions. However, the CMA case exhibits significantly higher MSPs than the other two fuel and PC coproduction cases due to the additional costs associated with converting microalgae PC to meat alternatives. As depicted in Fig. 2(g), maintaining the MSPs below the cost of conventional fuel and chicken meat appears infeasible at present. Nevertheless, GHG emissions can be kept below those of conventional fuel and chicken meat up to a potential fuel production threshold of roughly 4.2 billion GGE.

For validation purposes, this study's MSPs and GHG emissions are benchmarked against those from other literature.[9–11] The comparison shows that MSPs and GHG emissions are all within comparable ranges in similar cases to other studies. However, this study provides a broader range of MSP and GHG emissions by considering saline microalgae cultivation and conversion across the U.S., rather than focusing on specific cases. Detailed comparison can be found in Table S18 in the ESI.†

A biorefinery-level analysis is used to present the primary results of this study, avoiding arbitrary allocation and evaluation based on a specific main product. However, to compare with other studies, MSP per GGE of fuel production by accounting for PC selling price credits and GHG emissions per MJ of fuel and per kg of PC production by using economic allocation approach are detailed in Section 6 of the ESI.† The analysis shows that the MSP of fuel production in the fuel and PC coproduction scenarios is lower than in the fuel-only scenario but remains higher than conventional fuel production. For GHG emissions per MJ of fuel production, using the

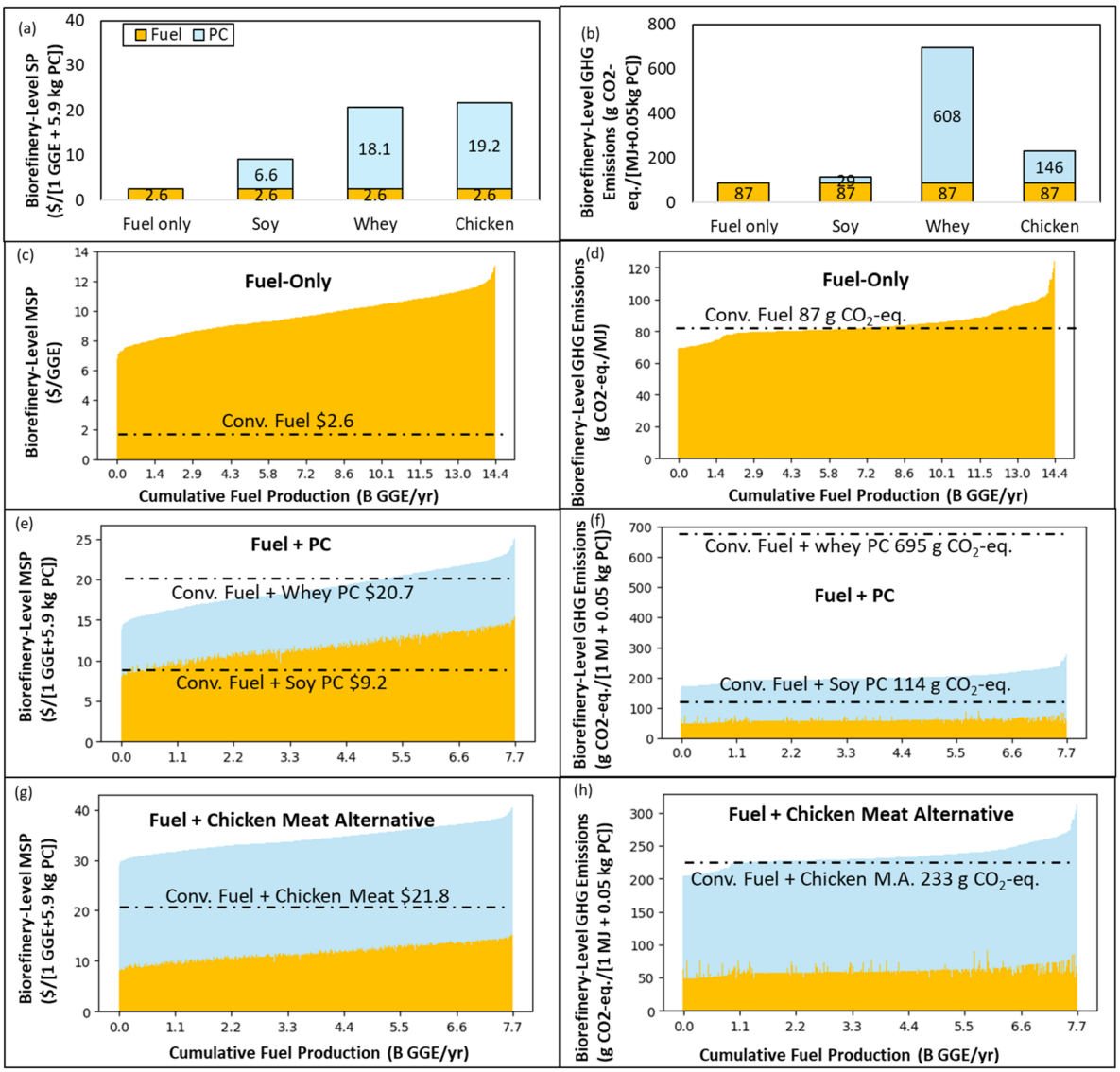

Fig. 2 Biorefinery-level (a) SP and (b) GHG emission benchmark for conventional fuel-only, conventional fuel plus PC for soybean PC, fuel plus PC for whey PC, and fuel plus PC for chicken meat cases, (c) MSPs and (d) GHG emissions for microalgal fuel-only case, (e) MSPs and (f) GHG emissions for microalgal fuel plus PC for soybean/whey PC case without market limits, and (g) MSPs and (h) GHG emissions for microalgal fuel plus PC for chicken meat case without market limit. Figures (c) to (h) are sorted in ascending order of their respective biorefinery MSP or GHG emissions.

economic allocation method, all weighted-average GHG emissions are lower than fossil fuels. In addition, GHG emissions are compared based on the production of 1 kg of digestible protein between biorefinery and conventional systems. The whey PC from the biorefinery shows significantly lower weighted-average GHG emissions than conventional whey PC; the chicken meat alternative is slightly higher than conventional chicken minus processing burdens; and the soy PC from the biorefinery exhibits higher emissions than conventional PC. These results align with findings from the biorefinery-level analysis. In addition, the MSP and GHG emission breakdown show that feedstock has the largest contribution to both MSP and GHG emissions, and detailed information can be found in Section 7 in the ESI.†

MAC

This section examines the trade-offs between SPs and GHG emissions using MAC. Electricity consumption is a key contributor to GHG emissions as discussed in the previous section, and as a result, this section also investigates MAC variations under different levels of grid electricity GHG intensity. Fig. 3 demonstrates the MAC in the fuel-only case and the fuel and protein coproduction cases within the respective benchmarked protein product market limits (soybean PC, whey PC, and chicken meat) using different carbon-intensive electricity mixes.

Electricity consumption is one of the main factors affecting GHG emissions. The GHG intensity of the U.S. electricity grid has declined by 45% between 2011 and 2024, which may further

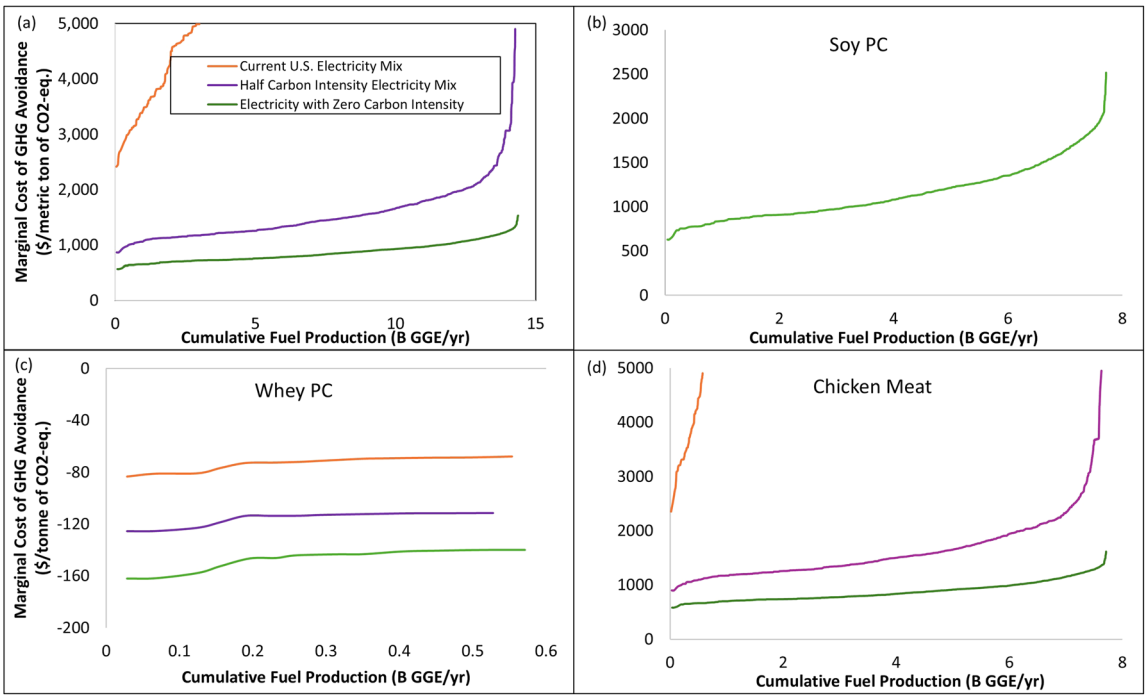

Fig. 3 MAC for (a) fuel-only, (b)–(d) fuel and PC production for benchmarking soybean PC, for whey PC, and for chicken meat cases within their respective market limits. Note: only sites with GHG emissions lower than those from their conventional fuel and PC production are included. Fuel-only and fuel and PC production for benchmarking chicken meat cases are capped with a $5000 per tonne *y*-axis limit. This is because when the MAC values are sorted in ascending order, the MAC in the current electricity scenario produces very large numbers at some sites, making it difficult to distinguish between the three scenarios when the MAC values are low.

decrease. These factors necessitate a sensitivity analysis around grid emission intensity. By using electricity at half the GHG intensity of the baseline and employing electricity with zero carbon intensity, the scenarios can achieve a substantial reduction in the MAC, as depicted by the purple and green lines in Fig. 3. While the SP is relatively stable with renewable energy according to U.S. EIA's future electricity projections, GHG emissions can be significantly lowered with less carbon-intensive energy sources. The reduction is due to the use of electricity with lower carbon intensity in both microalgae cultivation and biorefinery processes, as well as upstream processes like nutrient fertilizer production utilizing more renewable energy. However, it is notable that in a scenario with a carbon intensity half of the current electricity grid or a electricity grid with zero carbon intensity scenario, some CO_2 emission sources may no longer exist or the CO_2 concentration from these sources may be much lower, potentially increasing the electricity demand for CO_2 capture and transport. The increase in electricity consumption for CO_2 capture and transport in a less carbon-intensive electricity scenario has not been incorporated into this study, and further research is needed. The detailed GHG emissions for each case can be found in Section 9 in the ESI.†

Various sources recommend carbon price limits for carbon capture and storage ranging from $80 to $200/tonne CO_2 avoidance.[47–49] If a nominal target of $200 per tonne is provided, setting it as the threshold for MAC, the findings suggest that only the coproduction of fuel and PC for whey PC, can meet the cost across all sites with different levels of carbon-intensive electricity, influenced by whey PC's high market value and its significant GHG emissions. The cost is not achievable for the other three cases using the current U.S. electricity mix. Although the fuel-only case can achieve lower GHG emissions than conventional fuels, the MAC for the fuel-only case under current U.S. electricity inputs fails to meet the carbon cost primarily due to high MSP values ranging from $6.7 to $13.0 per GGE. No MAC value is illustrated for the coproduction of fuel and PC for soybean PC when using the current U.S. electricity mix, as GHG emissions consistently exceed those from conventional fuel and soybean PC production under current U.S. electricity sourcing assumptions. This renders the coproduction of algal PC to replace soybean PC impractical, especially given the lower energy and nutrient consumption in soybean PC production. Additionally, achieving the carbon cost for fuel and PC production for chicken meat is not feasible under current U.S. electricity inputs, primarily due to the high MSPs arising from the elevated costs associated with processing CMAs.

As shown in Fig. 3 (a), (b), and (d) the MACs for fuel-only as well as fuel and PC coproduction for soybean PC and chicken meat remain unable to achieve $200/tonne cost, even with carbon neutral electricity, despite significant reductions. However, from a development perspective, as arable land becomes increasingly limited for soybean cultivation and chicken farming due to population growth—even if the carbon price threshold remains unchanged—the SP benchmarks for soybean PC and chicken meat will rise, potentially bringing

MAC values below the current carbon price threshold. In the short term, however, arable land may not yet be a limiting factor. Current strategies to achieve carbon price threshold should focus on further reducing major cost and environmental hotspots by increasing biomass productivity, recycling or reducing nutrient use, and minimizing energy consumption.

Freshwater consumption and land use

Table 1 summarizes freshwater consumption, land use, market prices, and GHG emissions for 1 tonne of digestible protein. Saline algae, requiring no freshwater and significantly less land due to its high productivity. Land use calculations for poultry and whey PC consider the feed allocated for raising chickens and cows. Notably, the MBSP for algae is used to represent SP, although it should be lower than SP.

Carbon emissions resulting from LUC are also discussed here to illustrate how this factor can influence the final GHG emission results. The carbon emissions from DLUC are relatively minor when compared to the biorefinery-related GHG emissions from the four cases, which can be explained by the site selection criteria in the BAT model. The DLUC emissions are calculated to range from −1.83 to 9.33 g CO_2-eq. per MJ, averaging 1 g CO_2-eq. per MJ. The probability of original land use in each site and the calculated emissions from DLUC can be found in the SI. Nonetheless, the carbon emissions from ILUC of microalgal biorefineries and the carbon emissions from LUC of conventional soybean PC, whey PC, and chicken meat production exhibit considerable variability, depending on different assumptions. Including ILUC carbon emissions could markedly elevate GHG emissions under certain conditions as discussed in Section 4 in the ESI.† This study considers the GHG emissions from conventional PC and chicken meat production for benchmarking biorefinery-level emissions: 0.05 kg of PC is produced per MJ of fuel, and emissions associated with LUC of conventional PC and chicken meat can be significant, as indicated by the LUC emissions per kg of digestible protein in Table S16 in the ESI.† While LUC carbon emissions could significantly impact overall GHG emission figures, quantifying these variations is beyond this work's scope.

In summary, from a cost perspective, saline microalgal biorefinery for fuel-only production is currently not economically feasible, as its price exceeds that of conventional fuels. Incorporating protein coproducts into the biorefinery process can help address this issue, particularly when benchmarked against high-value products like whey PC. This benchmark requires careful consideration, as whey PC is derived from liquid whey, a cheese byproduct, and is only feasible when demand exceeds supply. Specifically, using microalgal protein coproduct to replace whey PC is only feasible when liquid whey cannot meet the demand for whey PC, necessitating an alternative to fill the supply gap. Furthermore, the protein coproduct benchmark does not improve the overall MSP performance when compared to lower-priced conventional products, such as soy PC. In addition, the study finds that the chicken meat alternative produced from protein coproducts is priced higher than conventional chicken meat. This conclusion, however, is subject to uncertainties due to price variations in chicken meat across different locations and times, as well as the potential for reduced processing costs for vegan meat with advancements in technology and economies of scale. Uncertainty regarding the future market for protein makes it difficult to predict the potential future value of algae-based protein products.

From an environmental impact perspective, three main factors are considered in this study: GHG emissions, GHG emissions from LUC, and freshwater usage. WSF will be discussed separately in the spatially explicit MSPs, GHG emissions, and WSF section since it is location based. Fuel-only production from a microalgal biorefinery can achieve lower GHG emissions compared to conventional fuels. Incorporating a protein coproduct may not further reduce GHG emissions if benchmarked against a more efficient conventional protein product, such as soy PC. Nutrient and energy consumption are the primary contributors to GHG emissions in both algae and soybean cultivation, with soybeans requiring significantly less nutrient and energy input. However, soybeans are typically grown on highly productive farmland and have a significantly lower protein yield per unit area compared with microalgae. These factors mean that replacing soybean with microalgae could reduce LUC effects, including deforestation. Additionally, the biorefinery-level GHG emissions from the coproduction of fuel and protein coproduct are comparable to those of the chicken meat benchmarking case. In this study, the GHG emissions from chicken meat production fall on the lower end of the values reported in the literature,[57] suggesting that benchmarking against chicken meat may be more plausible under certain circumstances. Furthermore, the freshwater consumption in saline microalgal biorefinery is much lower than that from other biomass benchmarks.

Table 1 Water, land use, market price, and GHG emissions comparison per tonne of digestible protein

Biorefinery bio-coproducts	Freshwater use[a] (m^3)	Land use (m^2 per year)	SP ($)	GHG emissions (kg CO_2-eq.)
Soy PC	131	2980	2120	1120
Whey PC	250	1850	6090	24 300
Chicken meat	259	9250	5090	2270[b]
Saline algae for fuel-only case in this study	0	226	1650–3060	1140–2630
References	27	This study, 50 and 51	This study and 52–56	This study and 27

[a] Freshwater use values are obtained from GREET model. [b] CMAs contain 30% of algal biomass by weight, and as a result, 1 kg of protein coproduct can be used to produce 3.3 kg of meat alternatives.

The MAC results suggest that electricity grid transitions could significantly reduce GHG emissions. However, the reduction alone cannot bring the MAC below the nominal carbon price threshold. The most promising direction for advancing microalgal biorefineries lies in simultaneously increasing biomass yield, reducing nutrient and energy consumption, and developing high-value products with GHG emissions reductions. Further research is needed on meat alternative benchmarks because: (1) microalgal PC can serve as an ingredient for various types of meat alternatives, such as beef, pork, and lamb, which have higher prices and GHG emissions compared to chicken meat; and (2) the market for meat alternatives is relatively new, with significant uncertainties. Additionally, other high-value protein coproduct benchmarks with smaller market sizes, such as pharmaceutical and cosmetic products, deserve further exploration. Their high value and potential GHG emission benefits could position them as feasible benchmarks. Furthermore, their smaller market sizes could complement larger markets, such as meat alternatives, creating a balanced and diversified portfolio of protein coproduct opportunities.

Correlation between total dissolved solid (TDS) and MSPs and GHG emissions

Utilizing saline microalgae can mitigate water stress without substantially impacting the overall MSPs and GHG emissions across cases mainly due to the energy efficient FO unit. Fig. S12 in the ESI† demonstrates that the relationships between TDS and MSPs and GHG emissions are not strong, suggesting that switching from freshwater to saline water does not dramatically affect MSPs and GHG emissions. Yet, an increase in TDS could raise GHG emissions and MSPs, with a more pronounced correlation between TDS and GHG emissions than between TDS and MSPs. As mentioned in section MAC, electricity significantly contributes to GHG emissions but not to MSPs, which explains the stronger correlation between total TDS and GHG emissions due to the increased electricity consumption associated with higher TDS levels.

The relationship between MSPs and GHG emissions, and other parameters, is explored using Pearson and Spearman correlations, utilizing data from BAT, TEA, and LCA compiled in an Excel file in the ESI.† When the Pearson or Spearman correlation coefficient exceeds 0.9 or drops below −0.9, with a P value under 0.05%, a significant correlation is indicated. Analysis shows a negative correlation between biomass yield and MSPs, where Spearman correlation coefficients are consistently below −0.9 for all cases. However, no significant correlations are identified between other parameters and MSPs or GHG emissions.

Spatially explicit MSPs, GHG emissions, and WSF

Spatially explicit MSPs, GHG emissions, and WSF for the fuel-only case are illustrated in Fig. 4 to demonstrate the correlation between sustainability metrics and geographical locations. The map distinguishes three major regions: Southeast (Florida and Georgia), South Central (Texas and Louisiana), and Western (California and Arizona). Southeast has the lowest

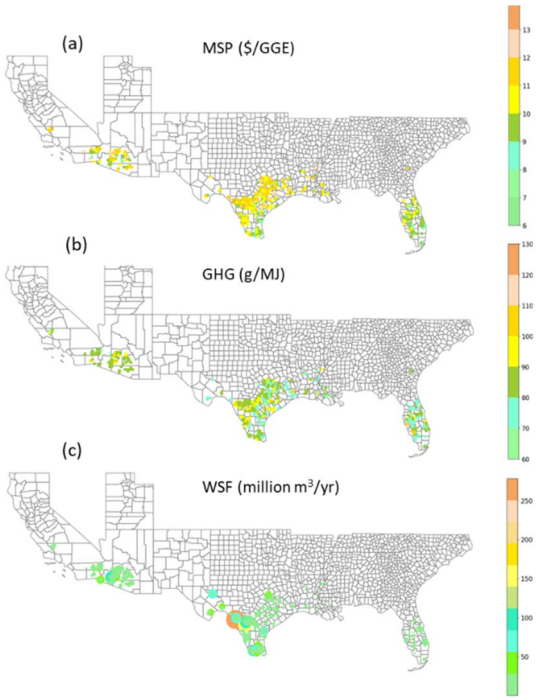

Fig. 4 (a) Minimum selling price ($/GGE), (b) greenhouse gas emissions (g CO_2-eq. per MJ), and (c) water scarcity footprint (million m^3 per year).

average MSPs due to relatively high biomass yield. GHG emissions, however, do not show a clear geographical trend, as the primary contributors – total electricity consumption and nutrient usage – do not vary significantly by location. Electricity consumption in algae cultivation and dewatering constitutes the largest portion of the total electricity consumption in the fuel-only case. This does not vary significantly across locations on a per fuel energy basis because the factors contributing to total energy requirements are independent and relate to locations in different ways. For example, electricity requirements for paddlewheel mixing are fixed per area but vary with biomass productivity on a per fuel basis. Additionally, electricity demand increases in higher salinity cultivation areas. The Southeast displays the lowest average WSF due to its low TDS, low freshwater CF, and low saline water consumption (reduced evaporation due to high humidity). Spatially explicit TDS, freshwater CF, biomass productivity, and biomass yield can be found in Section 11 in the ESI.†

Conclusions

Saline microalgae exhibit the potential for achieving significant GHG emission reductions with a less GHG-intensive grid, which can also substantially reduce the MAC. This is because electricity consumption is one of the primary drivers of GHG emissions in algae cultivation and downstream processing. However, even with the carbon intensity of electricity reduces, the MAC remains above current carbon prices. Limiting factors for lowering the MAC are identified across the four cases: high MSPs for the fuel-only case, low SPs and GHG emissions from

conventional soybean PC production for the soybean PC benchmarking case, small market size of whey PC for the whey PC benchmarking case, and high processing cost of meat alternative production for the chicken meat benchmarking case. These findings suggest three promising research directions: (1) actively increasing biomass yield, (2) further reducing nutrient and energy consumption in the integrated system spanning feedstock production and HTL conversion, and (3) carefully selecting high-value protein coproduct targets with significant GHG emission reduction potential during the microalgal biorefinery design stage. Saline-water-based microalgae have high potential to address water stress, as the increase in electricity requirements for desalination is not significant. Moreover, microalgal open pond systems can be situated on non-arable land, while also requiring less land per unit of biomass production due to the high productivity of microalgae. LUC credits from bio-coproducts are not negligible, and merit further studies. Through spatially explicit analysis, the Southeast region of the United States is identified as an optimal location for algae production given its lower WSF and MSPs.

Data availability

Detailed descriptions of system design and key assumptions, process parameters for various life cycle stages, life cycle inventory data, detailed water scarcity footprint and land use change emissions, relationships among different metrics, and validation with other studies are available in the ESI† Word document. Additional Pearson and Spearman correlation coefficients between different metrics are available in the ESI† Excel spreadsheet.

Author contributions

Jingyi Zhang: conception, methodology, formal analysis, validation, investigation, writing – original draft, visualization. Yunhua Zhu: conception, methodology, formal analysis, investigation. Troy R. Hawkins: conception, funding acquisition, supervision, writing – review & editing. Bruno C. Klein: formal analysis, investigation, writing – review & editing Andre M. Coleman: formal analysis, investigation, writing – review & editing. Udayan Singh: investigation, writing – review & editing. Ryan Davis: funding acquisition, writing – review & editing. Longwen Ou: writing – review & editing. Yiling Xu: investigation, writing – review & editing. Saurajyoti Kar: software. Matthew Wiatrowski: investigation, writing – review & editing. Song Gao: investigation, writing – review & editing. Peter Valdez: investigation, writing – review & editing.

Conflicts of interest

There are no conflicts to declare.

Acknowledgements

This work was authored by the Argonne National Laboratory, managed by UChicago Argonne, LLC, under DOE Contract No. DE-AC02-06CH11357; National Renewable Energy Laboratory, operated by Alliance for Sustainable Energy, LLC, for the U.S. Department of Energy (DOE) under Contract No. DE-AC36-08GO28308; and Pacific Northwest National Laboratory, operated by Battelle under DOE Contract No. DE-AC05-76RL01830. Funding provided by the U.S. Department of Energy Office of Energy Efficiency and Renewable Energy Bioenergy Technologies Office. The views expressed in the article do not necessarily represent the views of the DOE or the U.S. Government. The U.S. Government retains and the publisher, by accepting the article for publication, acknowledges that the U.S. Government retains a nonexclusive, paid-up, irrevocable, worldwide license to publish or reproduce the published form of this work, or allow others to do so, for U.S. Government purposes. In addition, we are grateful for the support and guidance provided by Dan Fishman. We also extend our thanks to Jason Quinn, Braden Limb, and Troy Saltiel for their inputs regarding land use change emissions.

Notes and references

1 UNEP, *Governments Plan to Produce Double the Fossil Fuels in 2030 than the 1.5 °C Warming Limit Allows*. 2023.
2 United Nations, *The United Nations World Water Development Report 2023: Partnerships and Cooperation for Water*, 2023.
3 K. W. Chew, J. Y. Yap, P. L. Show, N. H. Suan, J. C. Juan, T. C. Ling, D.-J. Lee and J.-S. Chang, *Bioresour. Technol.*, 2017, **229**, 53–62.
4 S. K. Bhatia, S. Mehariya, R. K. Bhatia, M. Kumar, A. Pugazhendhi, M. K. Awasthi, A. E. Atabani, G. Kumar, W. Kim, S.-O. Seo and Y.-H. Yang, *Sci. Total Environ.*, 2021, **751**, 141599.
5 Y. Ghasemi, S. Rasoul-Amini, A. T. Naseri, N. Montazeri-Najafabady, M. A. Mobasher and F. Dabbagh, *Appl. Biochem. Microbiol.*, 2012, **48**, 126–144.
6 US EIA, *Anuual Energy Outlook 2023. Table 57. Components of Selected Petroleum Product Prices*, **https://www.eia.gov/outlooks/aeo/data/browser/#/?id=70-AEO2023&region=1-0&cases=ref.2023&start=2021&end=2050&f=Q&linechart=ref.2023-d020623a.3-70-AEO2023.1-0&map=ref.2023-d020623a.3-70-AEO2023.1-0&sourcekey=0**, (accessed 3/18, 2024).
7 M. Wang, A. Elgowainy, U. Lee, K. H. Baek, S. Balchandani, P. T. Benavides, A. Burnham, H. Cai, P. Chen, Y. Gan, U. R. Gracida-Alvarez, T. R. Hawkins, T.-Y. Huang, R. K. Iyer, S. Kar, J. C. Kelly, T. Kim, C. Kolodziej, K. Lee, X. Liu, Z. Lu, F. Masum, M. Morales, C. Ng, L. Ou, T. Poddar, K. Reddi, S. Shukla, U. Singh, L. Sun, P. Sun, T. Sykora, P. Vyawahare and J. Zhang, *Summary of Expansions and Updates in R&D GREET® 2023*, (No. ANL/ESIA-23/10), Argonne National Laboratory (ANL), Argonne, IL (United States), 2023, Available from **https://www.osti.gov/biblio/2278803**.
8 M. Wiatrowski, B. C. Klein, R. W. Davis, C. Quiroz-Arita, E. C. Tan, R. W. Hunt and R. E. Davis, *Biotechnol. Biofuels Bioprod.*, 2022, **15**, 8.

9 C. Quiroz-Arita, S. Shinde, S. Kim, E. Monroe, A. George, J. Quinn, N. J. Nagle, E. P. Knoshaug, J. S. Kruger and T. Dong, *Sustainable Energy Fuels*, 2022, **6**, 2398–2422.
10 L. Y. Batan, G. D. Graff and T. H. Bradley, *Bioresour. Technol.*, 2016, **219**, 45–52.
11 C. M. Beal, L. N. Gerber, D. L. Sills, M. E. Huntley, S. C. Machesky, M. J. Walsh, J. W. Tester, I. Archibald, J. Granados and C. H. Greene, *Algal Res.*, 2015, **10**, 266–279.
12 E. Gnansounou and J. K. Raman, *Appl. Energy*, 2016, **161**, 300–308.
13 M. Montazeri, L. Soh, P. Pérez-López, J. B. Zimmerman and M. J. Eckelman, *Biofuels, Bioprod. Biorefin.*, 2016, **10**, 409–421.
14 M. S. Wigmosta, A. M. Coleman, R. J. Skaggs, M. H. Huesemann and L. J. Lane, *Water Resour. Res.*, 2011, **47**, W00H04.
15 H. Xu, U. Lee, A. M. Coleman, M. S. Wigmosta, N. Sun, T. Hawkins and M. Wang, *Environ. Sci. Technol.*, 2020, **54**, 2091–2102.
16 R. H. Davis, R. Troy, A. Coleman, S. Gao, B. Klein, M. Wiatrowski, Y. Zhu, Y. Xu, L. Snowden-Swan, P. Valdez, J. Zhang, U. Singh and L. Ou, *Economic, Greenhouse Gas, and Resource Assessment for Fuel and Protein Production from Microalgae: 2022 Algae Harmonization Update*, NREL/TP-5100-87099, 2024, DOI: **10.2172/2318964**.
17 R. E. Davis, J. N. Markham, C. M. Kinchin, C. Canter, J. Han, Q. Li, A. Coleman, S. Jones, M. Wigmosta and Y. Zhu, *2017 Algae harmonization study: evaluating the potential for future algal biofuel costs, sustainability, and resource assessment from harmonized modeling*, National Renewable Energy Lab.(NREL), Golden, CO (United States), 2018, DOI: **10.2172/1468333**.
18 P. Collet, A. Hélias, L. Lardon, J. P. Steyer and O. Bernard, *Appl. Energy*, 2015, **154**, 1089–1102.
19 A. M. Coleman, J. M. Abodeely, R. L. Skaggs, W. A. Moeglein, D. T. Newby, E. R. Venteris and M. S. Wigmosta, *Algal Res.*, 2014, **5**, 79–94.
20 R. Davis, A. Coleman, and A. Badgett. Emerging Resources: Microalgae, Macroalgae, and Point-Source Carbon Dioxide Waste Streams, *Bioenergy Knowledge Discovery Framework (BEKDF)*. Oak Ridge National Laboratory (ORNL), Oak Ridge, TN (United States), 2024.
21 US EPA, *Greenhouse Gas Reporting Program (GHGRP)*. **https://www.epa.gov/ghgreporting**, (accessed 1/14, 2024).
22 J. Bauer, C. Rowan, A. Barkhurst, J. Digiulio, K. Jones, M. Sabbatino, K. Rose and P. Wingo, *NATCARB*, National Energy Technology Laboratory (NETL), Pittsburgh, PA, Morgantown, WV, 2018.
23 R. S. Middleton, A. F. Clarens, X. Liu, J. M. Bielicki and J. S. Levine, *Environ. Sci. Technol.*, 2014, **48**, 11713–11720.
24 Geospatial Management Office. *Homeland Infrastructure Foundation-level Data (HIFLD)*. 2019.
25 H. Cai, J. Han, M. Wang, R. Davis, M. Biddy and E. Tan, *Biofuels, Bioprod. Biorefin.*, 2018, **12**, 815–833.
26 Y. Zhu, S. B. Jones, A. J. Schmidt, J. M. Billing, H. M. Job, J. R. Collett, S. J. Edmundson, K. R. Pomraning, S. P. Fox and T. R. Hart, *Microalgae Conversion to Biofuels and Biochemical via Sequential Hydrothermal Liquefaction (SEQHTL) and Bioprocessing: 2020 State of Technology*, Pacific Northwest National Lab (PNNL), Richland, WA (United States), 2021.
27 Y. Zhu, S. B. Jones, A. J. Schmidt, J. M. Billing, D. M. Santosa and D. B. Anderson, *Algal Res.*, 2020, **51**, 102053.
28 K. I. Al-Malah, *Aspen Process Economic Analyzer (APEA).* Hoboken, NJ, 2016.
29 Argonne National Laboratory, *GREET Model* 2022.
30 G. F. Institute, *Reducing the Price of Alternative Proteins*, 2021.
31 G. Philis, E. O. Gracey, L. C. Gansel, A. M. Fet and C. Rebours, *J. Cleaner Prod.*, 2018, **200**, 1142–1153.
32 USDA, *Whey Protein Concentrate (WPC)*, **https://www.ams.usda.gov/sites/default/files/media/Whey%20Protein%20Concentrate%20TR.pdf**, (accessed 10/3, 2022).
33 H. Aguirre-Villegas, F. Milani, S. Kraatz and D. Reinemann, *Trans. ASABE*, 2012, **55**, 613–627.
34 J. Bacenetti, L. Bava, A. Schievano and M. Zucali, *J. Food Eng.*, 2018, **224**, 139–147.
35 D. Kim, G. Thoma, D. Nutter, F. Milani, R. Ulrich and G. Norris, *Int. J. Life Cycle Assess.*, 2013, **18**, 1019–1035.
36 P. T. Benavides, H. Cai, M. Wang and N. Bajjalieh, *Anim. Feed Sci. Technol.*, 2020, **268**, 114607.
37 L. Grossmann, J. Hinrichs and J. Weiss, *Crit. Rev. Food Sci. Nutr.*, 2020, **60**, 2961–2989.
38 Y. Fu, T. Chen, S. H. Y. Chen, B. Liu, P. Sun, H. Sun and F. Chen, *Trends Food Sci. Technol.*, 2021, **112**, 188–200.
39 T. Ma, S. Sun, G. Fu, J. W. Hall, Y. Ni, L. He, J. Yi, N. Zhao, Y. Du and T. Pei, *Nat. Commun.*, 2020, **11**, 650.
40 A. S. Stillwell and M. E. Webber, *Water*, 2016, **8**, 601.
41 H. Nassrullah, S. F. Anis, R. Hashaikeh and N. Hilal, *Desalination*, 2020, **491**, 114569.
42 U. Lee, H. Xu, J. Daystar, A. Elgowainy and M. Wang, *Sci. Total Environ.*, 2019, **648**, 1313–1322.
43 C. Hong, J. A. Burney, J. Pongratz, J. E. M. S. Nabel, N. D. Mueller, R. B. Jackson and S. J. Davis, *Nature*, 2021, **589**, 554–561.
44 H. Eggleston, L. Buendia, K. Miwa, T. Ngara and K. Tanabe, *2006 IPCC guidelines for national greenhouse gas inventories*, 2006, Available from **https://www.ipcc-nggip.iges.or.jp/public/2006gl/**.
45 D. Quiroz, J. M. Greene, B. J. Limb and J. C. Quinn, *Environ. Sci. Technol.*, 2023, **57**, 11541–11551.
46 S. Smetana, Personal Communication, 2022.
47 Clean air task force, Carbon Capture Provisions in the Inflation Reduction Act of 2022, **https://cdn.catf.us/wp-content/uploads/2022/08/19102026/carbon-capture-provisions-ira.pdf?_gl=1*1jv95ce*_gcl_au*MTY4NTA1MDM5MC4xNjk2MzQzOTU1**, (accessed 1/6/2025).
48 Sandbag, Carbon Price Viewer, **https://sandbag.be/carbon-price-viewer/**(accessed 1/5, 2024).
49 J. E. Stiglitz, N. Stern, M. Duan, O. Edenhofer, G. Giraud, G. M. Heal, E. L. La Rovere, A. Morris, E. Moyer, M. Pangestu, and P. R. Shukla. *Report of the High-Level Commission on Carbon Prices*, 2017.

50 USDA, *United States Soybean Area, Yield and Production*, **https://ipad.fas.usda.gov/countrysummary/Default.aspx?id=US&crop=Soybean**, (accessed 5/14, 2024).
51 USDA, *United States Corn Area, Yield and Production*, **https://ipad.fas.usda.gov/countrysummary/Default.aspx?id=US&crop=Corn**, (accessed 5/14, 2024).
52 G. V. Research, *Protein Ingredients Market Size, Share & Trends Analysis Report By Product (Plant Proteins, Animal/Dairy Proteins, Microbe-based Proteins, Insect Proteins), By Application, By Region, And Segment Forecasts, 2021 - 2028*, **https://www.grandviewresearch.com/industry-analysis/protein-ingredients-market**, (accessed 10/1, 2022).
53 G. V. Research, *Whey Protein Market Size, Share & Trends Analysis Report By Type (WPI, WPC, WPH), By Application (Sports Nutrition, Dietary Supplements, Beverages), By Region, And Segment Forecasts, 2022 – 2030*, **https://www.grandviewresearch.com/industry-analysis/whey-protein-market** (accessed 10/1, 2022).
54 USDA, *Dairy Market Statistics 2021 Annual Summary*, 2021.
55 OECD, Food and A. O. o. t. U. Nations, *OECD-FAO Agricultural Outlook 2020-2029*, 2020.
56 *IndexBox, World - Chicken Meat - Market Analysis, Forecast, Size, Trends and Insights*, **https://www.indexbox.io/blog/global-chicken-meat-market-2023-key-insights/**, (accessed 1/14, 2024).
57 D. Skunca, I. Tomasevic, I. Nastasijevic, V. Tomovic and I. Djekic, *J. Cleaner Prod.*, 2018, **184**, 440–450.

